VIP Nanoparticle Chains

DOI: 10.1002/anie.201203088

Unconventional Chain-Growth Mode in the Assembly of Colloidal Gold Nanoparticles**

*Hong Wang, Liyong Chen, Xiaoshuang Shen, Liangfang Zhu, Jiating He, and Hongyu Chen**

The assembly of nano-objects is a fundamental step toward the development of functional nanodevices. For the optimization of properties and functions, it is important to achieve structural precision. Electronic and plasmonic coupling between metallic nanoparticles (NPs) has been known to give novel electronic and optical properties.[1] Such coupling is critically dependent on structural parameters, such as interparticle spacing[2] and the spatial organization of individual NPs. In comparison to higher-order nanostructures, one-dimensional (1D) NP chains are more convenient building blocks for circuits in nanoelectronics, optoelectronics,[3] and biosensors.[4] Minimizing structural irregularity is essential: a large gap may break the coupling along a chain, and branching may cause a short circuit.

A popular approach for assembling NPs is to utilize templates, such as biomolecules,[5] polymers,[6] and lithographically created patterns.[7] A general problem of these methods is the lack of means to achieve close packing of the NPs in a chain and avoid irregular gaps. On the other hand, simple colloidal aggregation can bring NPs closely together, with short and regular gaps dictated by their ligand layers.[8] However, colloidal-assembly methods based on random aggregation are generally difficult to control. Thus there is great interest to devise controlling methods. Linear assembly of NPs has been achieved by exploiting the anisotropic ligand organization on Au nanorods,[9] or the phase segregation of immiscible ligands on nanospheres.[10] In addition, intrinsic interactions of NPs, such as dipole–dipole interactions[11] or electrostatic charge repulsion,[12] have been proposed to explain the 1D aggregation of NPs. Despite these advances, it remains a great challenge to program the behavior of NPs for a longer-range order, for example, in terms of preventing branching and controlling cross-sectional width.

The aggregation of colloidal NPs in a 3D space can be compared to the polymerization of organic monomers.[9d,13] The general characteristic of step-growth polymerization is that all monomers and oligomers are reactive. Their random combination quickly consumes monomers, so that the later-stage reaction mostly involves the coupling of oligomers (i.e., *m*-to-*n* coupling; *m* and *n* are the numbers of structural units in the chain). If this reaction is inefficient, few long chains will be obtained. In contrast, in chain-growth polymerization the active species (e.g., radicals or initiators) are limited in concentration, thus making the coupling between monomers (1-to-1 coupling) unfavorable. The excess monomers can continuously react with the active species and supply the chain growth through 1-to-*n* coupling.

Because all NPs in a colloid are capable of aggregating, their "polymerization" tends to follow the step-growth mode. Once monomers are depleted, the *m*-to-*n* coupling of larger clusters becomes more difficult and less selective, leading to branches and irregularities. Hence, obtaining long chains (> 30 NPs in length) is very difficult. Here, we report the use of polymer shells to assist the 1D assembly of colloidal AuNPs (Figure 1). The system is unique in that the aggregation of NPs follows a mode that is similar to chain-growth polymerization and gives long chains up to 300 NPs in length. The monomers that are used are AuNPs encapsulated by polystyrene-*block*-poly(acrylic acid) (AuNP@PSPAA, Figure 1b). Induced by the structural transformation of the polymer micelles from spheres to cylinders, the embedded AuNPs are forced to form chains. We provide evidences that the end-on

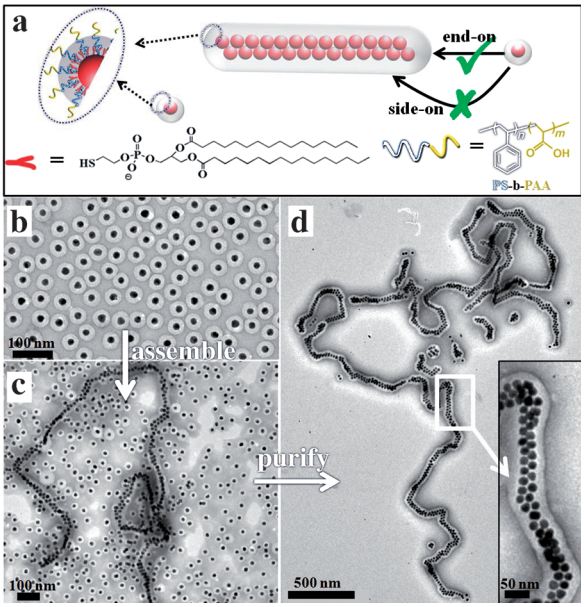

Figure 1. a) Schematics illustrating the 1D assembly of AuNP@PSPAA assisted by the sphere-to-cylinder transformation of polymer micelles. b–d) TEM images of AuNP@PSPAA monomers (b) and double-line chains before (c) and after (d) purification.

[*] H. Wang, L. Chen, X. Shen, L. Zhu, J. He, Prof. H. Chen
Division of Chemistry and Biological Chemistry
Nanyang Technological University
21 Nanyang Link, Singapore 637371 (Singapore)
E-mail: hongyuchen@ntu.edu.sg
Homepage: http://www.ntu.edu.sg/home/hongyuchen/

[**] The authors thank the MOE (ARC 13/09) and NRF (CRP-4-2008-06) of Singapore for financial supports.

Supporting information for this article is available on the WWW under http://dx.doi.org/10.1002/anie.201203088.

aggregation (1-to-*n* coupling) is more favorable than the monomer aggregation (1-to-1 coupling), thus setting the stage for continued chain growth.

The AuNP@PSPAA monomers were synthesized as previously reported.[14] Citrate-stabilized AuNPs ($d = 16$ nm) were first functionalized with a hydrophobic ligand, 1,2-dipalmitoyl-*sn*-glycero-3-phosphothioethanol. The amphiphilic polymer PSPAA was then self-assembled on the NP surface to form a uniform shell, with poly(acrylic acid) (PAA) blocks dissolved in water (Figure 1a). The core–shell NPs were isolated by centrifugation to completely remove the excess PSPAA.[15] To induce 1D assembly, the purified monomeric NPs were then redispersed in a DMF–water mixture ($V/V = 7{:}3$).[16] To facilitate the shape transformation of the polymer shells, the mixture was incubated at 70 °C after addition of HCl (5 mM). Though the glass transition temperature of neat polystyrene (PS) is above 100 °C, under our conditions, the PS domains were swollen by DMF. Thus, they are quite plastic, even at lower temperatures (50–70 °C). After two hours, the solution was diluted with a large amount of aqueous NaOH to neutralize the acid and remove DMF from the polymer shells. The PSPAA shells solidified after deswelling,[16] and the products were isolated by centrifugation and characterized by transmission electron microscopy (TEM).

In the resulting product, most of the AuNPs were in the form of double-line chains and the excess unreacted monomers (Figure 1c).[15] All of them still have a polymer shell covering their surface. Given their large difference in size and weight, the long chains were easily enriched by differential centrifugation (Figure 1d).[13,17] Most of the chains were very long, with a typical length of 30–200 NPs, but a few short chains were also observed. Nevertheless, their width was remarkably uniform of almost exactly two NPs. Unlike the typical 1D aggregates of NPs,[11a,12c,18] branching was rarely observed in our products. The long and wavy chains often contain kinks, probably resulting from their Brownian motion or the collapsing of their 3D conformation upon drying.

The ultralong chains must have been formed by extensive aggregation, which is counterintuitive, considering that a lot of monomers still remained. Random and equivalent coupling of monomers would have followed the step-growth mode, but obviously all of the monomers did not participate equally in the aggregation. Previously, we studied the random aggregation of ligand-coated AuNPs by using polymer encapsulation, only to preserve the resulting aggregates after their formation.[12c,18] In the current study, the monomers already have polymer shells before participating in the aggregation. Because the resulting ultralong chains were unique, it appeared that the polymer shells played important roles. In particular, the conversion of core–shell NPs to long cylindrical aggregates is reminiscent of the transformation of spherical PSPAA micelles to cylindrical ones upon addition of acid.[19] Most importantly, the uniform width of exactly two NPs can hardly be explained by any other mechanism except the transverse confinement provided by the polymer shells.

A prominent feature of the chains was that the AuNPs were in direct contact with each other (Figure 1d, inset), which cannot be achieved by simple aggregation of the core–shell NPs. Because the polymer layers between the two cores have to move away, the assembly process must have involved the reorganization of the polymer shells. It should be noted that the volume of the polymer shell on an aggregate is always less than the total volume of the initial shells on the constituent AuNPs (by about 20% for the double-line chains).[15] This excess polymer was found in the form of free (without AuNP) polymer spheres, cylinders, and vesicles, which have been removed during the centrifugation step (see the Supporting Information for the samples before isolation). Thus, the assembly involved two distinct processes: the aggregation of the core–shell NPs and the reorganization of the PSPAA shells.

Actually, the conditions of our experiments have been optimized to facilitate both processes. The PAA blocks were protonated at a low pH value, thus reducing the surface charges on the monomer NPs. With less charge repulsion among the PSPAA micelles, their aggregation was a favourable process driven by van der Waals and hydrophobic interactions among the PS domains.[19b] The kinetic motion of the NPs at high temperature helped to overcome the mutual charge repulsion and thus promoted aggregation.[19a,b,20] On the other hand, the mobility of the polymer domains was improved at high temperature and also by the swelling of the PS blocks in the DMF-rich solvent. As shown by control experiments, in the absence of HCl and at 70 °C, the core–shell NPs did not aggregate; their polymer shells mostly remained unchanged.[15] Similarly, at 30 °C, the acid only caused slight aggregation of the core–shell NPs. In the few aggregates that we observed, the monomers did not fully merge and roughly retained their spherical shape.[15]

Because it was known that solvent quality can greatly influence the mobility as well as the final morphologies of PSPAA micelles,[19a,b,21] we studied the influence of the solvent on the assembly. When the DMF/water ratio was increased from 7:3 to 6:1, the obtained product consisted mostly of ultralong single-line chains (up to 300 NPs in length) in addition to excess monomers (Figure 2c). The decrease in chain width was clearly associated with the polymer shells: Because DMF was still the dominant component in the solvent, direct aggregation of NPs cannot explain the dramatic change in products. After the excess monomers were removed, the purified product was highly uniform with only few defects, such as branches and additional AuNPs attached on the sides (Figure 3a). Though the long chains were stacked across each other in the dried sample, their shells did not fuse together. With further increase of the DMF/water ratio to 9:1, however, the resulting product was less defined (Figure 2a). There was more frequent occurrence of branches and misplaced AuNPs at the sides. It was also apparent that the crossed chains were able to fuse together, thus causing the chains to entangle (Figure 2a). Such entanglement can be more clearly seen in the purified products (Figure 2b).[15] On the other hand, when the DMF/water ratio was decreased to 2:3, the aggregation changed dramatically to the step-growth mode, as indicated by the disappearance of monomers (see Figure 2d for a sample before purification). The products were still chain-like with an irregular width of 1–3 NPs, but long chains (> 30 NPs in length) were not found.

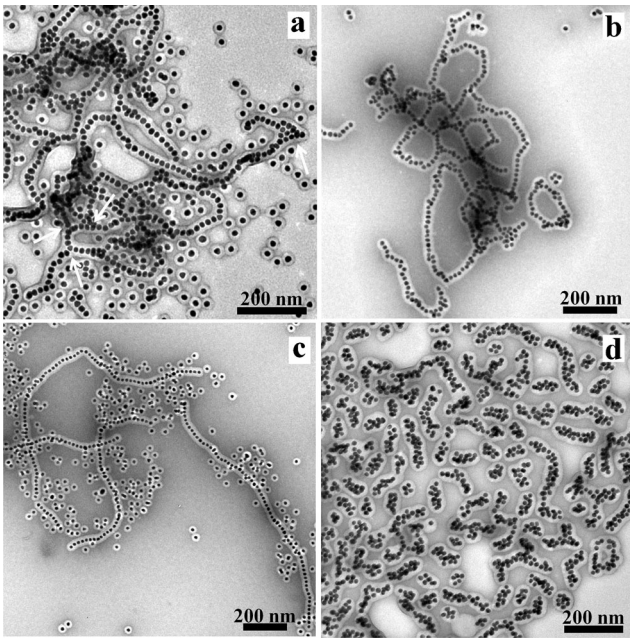

Figure 2. TEM images showing the influence of the DMF/H_2O ratio on the assembly products: a, b) $V_{DMF}/V_{H2O} = 9{:}1$, before (a) and after (b) purification (the arrows indicate fusion of polymer shells). c) $V_{DMF}/V_{H2O} = 6{:}1$, before purification. d) $V_{DMF}/V_{H2O} = 2{:}3$, before purification.

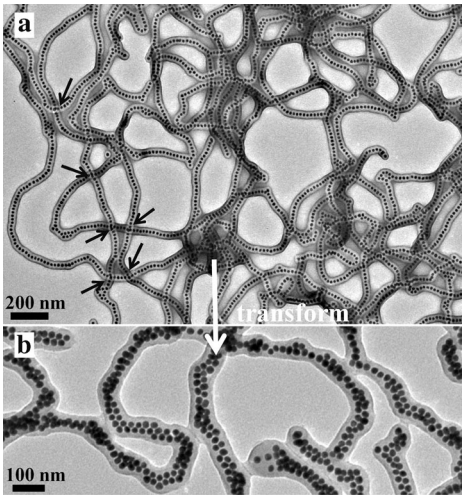

Figure 3. TEM images showing a) the single-line chains isolated from the sample in Figure 2c (the arrows indicate the absence of polymer fusion), b) the double-line chains formed from the single-line chains in (a) through treatment in an acidic $V_{DMF}/V_{H2O} = 7{:}3$ solution and heating the mixture at 70°C for one hour.

The formation of single-line chains can be understood from the sequential 1-to-*n* coupling between a chain and monomers, but the formation of double-line chains is more complex. In particular, the question is whether the transverse confinement provided by a polymer shell is a kinetic or thermodynamic factor. That is, does the polymer shell facilitate the end-on aggregation, or does it simply make the double-line chains more stable? To answer this question, we carried out the following set of experiments. Single-line chains were first prepared in $V_{DMF}/V_{H2O} = 6{:}1$ solution and purified (Figure 3a). They were then dispersed in $V_{DMF}/V_{H2O} = 7{:}3$ solution with HCl to favor the double-line chains. After incubation at 70°C for one hour, the isolated product showed mostly double-line chains, though sometimes they still had a few remaining single-line sections (Figure 3b). Thus, the double-line chains were indeed more stable in the $V_{DMF}/V_{H2O} = 7{:}3$ solution. Even if single-line chains were initially formed during the aggregation, they could be converted to the double-line chains. By further decreasing the DMF/H_2O ratio to 3:2, triple-line chains can be also obtained by this method, though they often contained more defects, for example, remaining single- and double-line sections.

Conversely however, when the double-line chains were first synthesized and then introduced into the conditions favoring single-line chains ($V_{DMF}/V_{H2O} = 6{:}1$ with HCl), the latter were not obtained. It appeared that the compression of the chains was easier than their elongation. This result highlighted the importance of the selectivity in the initial end-on aggregation: If monomers were somehow attached wrongly to the side of the chains, such an error could not be easily fixed because of the difficulty in reorganizing the NPs in the chains.

Under the typical temperature used (70°C), the aggregation went too fast for us to isolate the intermediates to confirm the end-on aggregation. Fortunately, as we lowered the temperature to 50°C ($V_{DMF}/V_{H2O} = 6{:}1$), we were able to identify a number of examples, in which a monomer just started to fuse with a chain (Figure 4a,b).[15] Apparently, the polymer at some newly formed junctions was solidified by deswelling before the monomers had enough time to fully merge with the chains. Among the 323 chains we surveyed, 146 of them contained gapped intermediates, including 121 cases of end-on 1-to-*n* coupling, 19 cases of end-on *m*-to-*n* coupling, and 6 cases of side-on 1-to-*n* coupling. The assembly errors were obviously more frequent than the typical results obtained at 70°C (Figure 2c and 3a). Never-

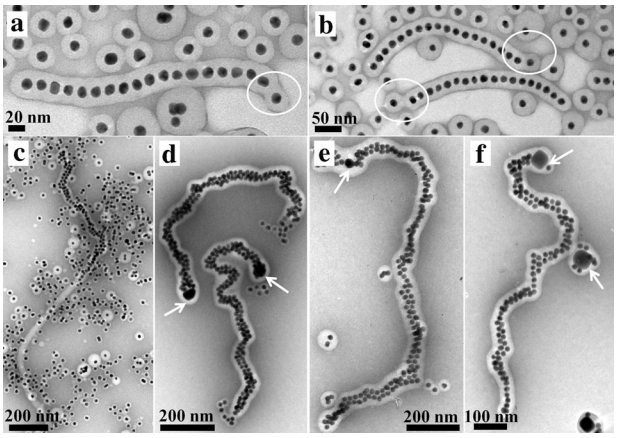

Figure 4. a, b) TEM images showing the intermediate species trapped at 50°C in $V_{DMF}/V_{H2O} = 6{:}1$ solution. c) TEM image showing that empty polymer cylinders grew on the end of double-line chains. d–f) large AuNP@PSPAA (40 nm and 30 nm) and AgNC@PSPAA were used as seeds to grow chains.

theless, these results indicated that end-on aggregation was a favored process.

We were not able to characterize the initial chain growth by UV/vis absorption for the following reasons. The chains constituted only a small population in the mixture and long chains only absorb in the near-infrared region.[9a] Moreover, with the current ligand, the plasmonic coupling between AuNPs was not strong enough to give prominent absorption peaks.[13]

Control experiments were carried out to further understand the assembly process. In one set of experiments, we first synthesized double-line chains; without stopping the reaction, excess amount of empty PSPAA micelles were added into the reaction mixture, so that the subsequent aggregation was dominated by the assembly of empty micelles. We found a number of examples of empty polymer cylinders growing on one end of the double-line chains (Figure 4c). We did not find any example of polymer cylinders growing on both ends of a chain. In another set of experiments, we used large NP@PSPAA (30 or 40 nm AuNPs or 45 nm Ag nanocubes (AgNCs)) as seeds to grow chains, so that the starting points could be identified. A small amount of seeds were first dispersed in $V_{DMF}/V_{H2O} = 7{:}3$ solution and treated with 2 mM HCl. Under the acidic conditions, the polymer shells of the seeds were destabilized, but they could not aggregate effectively because of their low concentration. After 30 minutes, a large amount of AuNP@PSPAA ($d_{Au} = 16$ nm) monomers were added to initiate the aggregation. The mixture was then heated at 70 °C for two hours. Large-seed NPs often occurred at the end of the resulting double-line chains (Figure 4d–f). It was much rarer for chains to grow on two sides of a seed (Figure 4e). But even in this case, one side grew much longer than the other, thus suggesting unequal growth. Some seeds had a few monomers merged to their surface (Figure 4f), but they did not develop into chains.

The 1D assembly of AuNP@PSPAA is both thermodynamically and kinetically favored. From the thermodynamic perspective, the morphologies of PSPAA micelles are governed by three major factors: a) the entropy of the coiled polymer in the PS domain limits the domain depth;[21b,22] b) the charge and steric repulsion among PAA blocks favor a high surface-to-volume ratio (S/V),[19] that is, individual spheres; and c) the polymer–solvent interfacial tension favors low S/V,[21d] that is, fused cylinders. The protonation of PAA blocks reduces their mutual charge repulsion, thus favoring cylinders. However, the overall S/V can only be slightly reduced when the aggregated core–shell NPs simply contact each other[23] (by 0.55–11.5% in Figure 4a,b). A more significant driving force can be achieved by fully merging the shells, thus removing their spherical outline and bringing the cores closely together.[15] Therefore, the thermodynamic stability of polymer cylinders impedes the formation of branches. During the formation of the double-line chains, the higher water content in the solvent reduces swelling and thus leads to higher polymer–solvent interfacial tension. This process provides a small but controllable driving force to reduce the S/V of the chains, leading to expansion of the chain width.

From the kinetic perspective, the ends of polymer cylinders are more active because of their high curvature,[24] thus favoring end-on aggregation. Moreover, both the chain and the monomers are negatively charged because of the PAA blocks on their surface. It is known that, for an incoming monomer, end-on aggregation to a chain is favored because the charge repulsion from the end is smaller than that from the side.[12c] Most importantly, in chain-growth mode the 1-to-n coupling is the dominant process, which is more selective than the m-to-n coupling between chains during the later stage of step-growth "polymerization".

In our system, the fact that a large amount of monomers remained after forming long chains is a strong indication for chain-growth mode. The main difference from the step-growth mode is that not all monomers were equally active toward aggregation. There are clear evidences for the unequal activation of the polymer shells: a) not all monomers participated in the aggregation; b) the ends have higher activity than the sides (intermediates in Figure 4a,b); c) the empty polymer cylinder only grew on one end of the double-line chain (Figure 4c); and d) the chains preferentially grew on one end of the seeds (Figure 4d–f).

In summary, we observed an unprecedented mode of "polymerization" in nanoparticle aggregation. This mode was essential for achieving high selectivity in the assembly of chains, thus reducing branching and other errors. We were able to obtain single-line chains of 300 nanoparticles in length and double-line chains of 200 nanoparticles. These ultralong chains, with uniform width and interpartical spacing, could be potentially useful as plasmonic waveguide and device component.

Received: April 22, 2012
Published online: July 18, 2012

Keywords: aggregation · chain-growth polymerization · double-line chains · nanoparticles · single-line chains

[1] a) Z. H. Nie, A. Petukhova, E. Kumacheva, *Nat. Nanotechnol.* **2010**, *5*, 15–25; b) Z. Y. Tang, N. A. Kotov, *Adv. Mater.* **2005**, *17*, 951–962; c) S. Srivastava, N. A. Kotov, *Soft Matter* **2009**, *5*, 1146–1156; d) N. J. Halas, S. Lal, W. S. Chang, S. Link, P. Nordlander, *Chem. Rev.* **2011**, *111*, 3913–3961.

[2] K. H. Su, Q. H. Wei, X. Zhang, J. J. Mock, D. R. Smith, S. Schultz, *Nano Lett.* **2003**, *3*, 1087–1090.

[3] a) S. A. Maier, M. L. Brongersma, P. G. Kik, S. Meltzer, A. A. G. Requicha, H. A. Atwater, *Adv. Mater.* **2001**, *13*, 1501–1505; b) S. A. Maier, P. G. Kik, H. A. Atwater, S. Meltzer, E. Harel, B. E. Koel, A. A. G. Requicha, *Nat. Mater.* **2003**, *2*, 229–232; c) C.-J. Wang, L. Huang, B. A. Parviz, L. Y. Lin, *Nano Lett.* **2006**, *6*, 2549–2553; d) T. Yatsui, Y. Ryu, T. Morishima, W. Nomura, T. Kawazoe, T. Yonezawa, M. Washizu, H. Fujita, M. Ohtsu, *Appl. Phys. Lett.* **2010**, *96*, 133106; e) Z. Zhu, W. Liu, Z. Li, B. Han, Y. Zhou, Y. Gao, Z. Tang, *ACS Nano* **2012**, *6*, 2326–2332.

[4] a) F. Favier, E. C. Walter, M. P. Zach, T. Benter, R. M. Penner, *Science* **2001**, *293*, 2227–2231; b) J. N. Anker, W. P. Hall, O. Lyandres, N. C. Shah, J. Zhao, R. P. Van Duyne, *Nat. Mater.* **2008**, *7*, 442–453.

[5] M. G. Warner, J. E. Hutchison, *Nat. Mater.* **2003**, *2*, 272–277.

[6] J. Y. Yuan, A. H. E. Muller, *Polymer* **2010**, *51*, 4015–4036.

[7] Q. H. Wei, K. H. Su, S. Durant, X. Zhang, *Nano Lett.* **2004**, *4*, 1067 – 1071.

[8] a) X. Shen, L. Chen, D. Li, L. Zhu, H. Wang, C. Liu, Y. Wang, Q. Xiong, H. Chen, *ACS Nano* **2011**, *5*, 8426 – 8433; b) G. Chen, Y. Wang, M. X. Yang, J. Xu, S. J. Goh, M. Pan, H. Y. Chen, *J. Am. Chem. Soc.* **2010**, *132*, 3644 – 3645; c) Y. Wang, G. Chen, M. Yang, G. Silber, S. Xing, L. H. Tan, F. Wang, Y. Feng, X. Liu, S. Li, H. Chen, *Nat. Commun.* **2010**, *1*, 87.

[9] a) Z. H. Nie, D. Fava, E. Kumacheva, S. Zou, G. C. Walker, M. Rubinstein, *Nat. Mater.* **2007**, *6*, 609 – 614; b) S. Z. Zhang, X. S. Kou, Z. Yang, Q. H. Shi, G. D. Stucky, L. D. Sun, J. F. Wang, C. H. Yan, *Chem. Commun.* **2007**, 1816 – 1818; c) Z. H. Nie, D. Fava, M. Rubinstein, E. Kumacheva, *J. Am. Chem. Soc.* **2008**, *130*, 3683 – 3689; d) K. Liu, Z. H. Nie, N. N. Zhao, W. Li, M. Rubinstein, E. Kumacheva, *Science* **2010**, *329*, 197 – 200; e) T. Chen, H. Wang, G. Chen, Y. Wang, Y. Feng, W. S. Teo, T. Wu, H. Chen, *ACS Nano* **2010**, *4*, 3087 – 3094.

[10] a) G. A. DeVries, M. Brunnbauer, Y. Hu, A. M. Jackson, B. Long, B. T. Neltner, O. Uzun, B. H. Wunsch, F. Stellacci, *Science* **2007**, *315*, 358 – 361; b) K. Nakata, Y. Hu, O. Uzun, O. Bakr, F. Stellacci, *Adv. Mater.* **2008**, *20*, 4294 – 4299; c) G. A. DeVries, F. R. Talley, R. P. Carney, F. Stellacci, *Adv. Mater.* **2008**, *20*, 4243 – 4247.

[11] a) Z. Y. Tang, N. A. Kotov, M. Giersig, *Science* **2002**, *297*, 237 – 240; b) K. Butter, P. H. H. Bomans, P. M. Frederik, G. J. Vroege, A. P. Philipse, *Nat. Mater.* **2003**, *2*, 88 – 91; c) S. Lin, M. Li, E. Dujardin, C. Girard, S. Mann, *Adv. Mater.* **2005**, *17*, 2553 – 2559; d) M. Klokkenburg, A. J. Houtepen, R. Koole, J. W. J. de Folter, B. H. Erne, E. van Faassen, D. Vanmaekelbergh, *Nano Lett.* **2007**, *7*, 2931 – 2936; e) L. Zhu, D. H. Xue, Z. X. Wang, *Langmuir* **2008**, *24*, 11385 – 11389; f) B. D. Korth, P. Keng, I. Shim, S. E. Bowles, C. Tang, T. Kowalewski, K. W. Nebesny, J. Pyun, *J. Am. Chem. Soc.* **2006**, *128*, 6562 – 6563; g) P. Y. Keng, I. Shim, B. D. Korth, J. F. Douglas, J. Pyun, *ACS Nano* **2007**, *1*, 279 – 292; h) Y. X. Hu, L. He, Y. D. Yin, *Angew. Chem.* **2011**, *123*, 3831 – 3834; *Angew. Chem. Int. Ed.* **2011**, *50*, 3747 – 3750.

[12] a) H. Zhang, K. H. Fung, J. Hartmann, C. T. Chan, D. Y. Wang, *J. Phy. Chem. C* **2008**, *112*, 16830 – 16839; b) H. Zhang, D. Y. Wang, *Angew. Chem.* **2008**, *120*, 4048 – 4051; *Angew. Chem. Int. Ed.* **2008**, *47*, 3984 – 3987; c) M. Yang, G. Chen, Y. Zhao, G. Silber, Y. Wang, S. Xing, Y. Han, H. Chen, *Phys. Chem. Chem. Phys.* **2010**, *12*, 11850 – 11860.

[13] X. J. Wang, G. P. Li, T. Chen, M. X. Yang, Z. Zhang, T. Wu, H. Y. Chen, *Nano Lett.* **2008**, *8*, 2643 – 2647.

[14] a) H. Y. Chen, S. Abraham, J. Mendenhall, S. C. Delamarre, K. Smith, I. Kim, C. A. Batt, *ChemPhysChem* **2008**, *9*, 388 – 392; b) M. X. Yang, T. Chen, W. S. Lau, Y. Wang, Q. H. Tang, Y. H. Yang, H. Y. Chen, *Small* **2009**, *5*, 198 – 202.

[15] See Supporting Information for details.

[16] L. H. Tan, S. X. Xing, T. Chen, G. Chen, X. Huang, H. Zhang, H. Y. Chen, *ACS Nano* **2009**, *3*, 3469 – 3474.

[17] G. Chen, Y. Wang, L. H. Tan, M. Yang, L. S. Tan, Y. Chen, H. Chen, *J. Am. Chem. Soc.* **2009**, *131*, 4218 – 4219.

[18] S. Xing, L. H. Tan, M. Yang, M. Pan, Y. Lv, Q. Tang, Y. Yang, H. Chen, *J. Mater. Chem.* **2009**, *19*, 3286 – 3291.

[19] a) L. F. Zhang, K. Yu, A. Eisenberg, *Science* **1996**, *272*, 1777 – 1779; b) C. Liu, G. Chen, H. Sun, J. Xu, Y. Feng, Z. Zhang, T. Wu, H. Chen, *Small* **2011**, *7*, 2721 – 2726; c) L. Zhang, A. Eisenberg, *Macromolecules* **1996**, *29*, 8805 – 8815.

[20] P. Bhargava, Y. Tu, J. X. Zheng, H. Xiong, R. P. Quirk, S. Z. D. Cheng, *J. Am. Chem. Soc.* **2007**, *129*, 1113 – 1121.

[21] a) L. F. Zhang, A. Eisenberg, *Science* **1995**, *268*, 1728 – 1731; b) Y. S. Yu, A. Eisenberg, *J. Am. Chem. Soc.* **1997**, *119*, 8383 – 8384; c) A. Choucair, A. Eisenberg, *Eur. Phys. J. E* **2003**, *10*, 37 – 44; d) Y. Yu, L. Zhang, A. Eisenberg, *Macromolecules* **1998**, *31*, 1144 – 1154.

[22] L. Zhang, A. Eisenberg, *J. Am. Chem. Soc.* **1996**, *118*, 3168 – 3181.

[23] Y. J. Kang, K. J. Erickson, T. A. Taton, *J. Am. Chem. Soc.* **2005**, *127*, 13800 – 13801.

[24] a) T. Smart, H. Lomas, M. Massignani, M. V. Flores-Merino, L. R. Perez, G. Battaglia, *Nano Today* **2008**, *3*, 38 – 46; b) H. Cui, Z. Chen, K. L. Wooley, D. J. Pochan, *Soft Matter* **2009**, *5*, 1269 – 1278.

